A Novel Energy Mapping Approach in CT-Based Attenuation Correction of PET Data Using Multi-Energy CT Imaging

H. Ghadiri, M.B. Shiran, M.R. Ay, *Member, IEEE,* H. Soltanian-Zadeh, *Senior Member, IEEE,* A. Rahmim, *Member, IEEE,* and H. Zaidi, *Senior Member, IEEE*

***Abstract*– A major source of potential pitfalls in CT-based attenuation correction (CTAC) of PET data is the use of integral mode of CT detectors in the presence of polychromatic x-rays resulting in limited information for determination of exact tissue content. The wide range of bone mineral contents and densities in the human body makes it difficult to map the CT number to Linear Attenuation Coefficient (LAC) at the PET energy when merely using one or two scaling factors. In this study we proposed an alternative approach in order to use energy sensitive CT imaging techniques as opposed to integrating CT imaging. The multi-energy strategy would promise significant improvements in tissue determination and leads to accurate energy mapping results in CTAC, which can be especially critical and useful in the presence of varying bone tissues. In order to accurately validate our method a novel bone model based on cortical and marrow mixtures is proposed. Furthermore, a two-step energy mapping algorithm is implemented. For validation, tomographic projections of phantom in five energy bin were acquired and reconstructed. The proposed energy mapping technique was used to estimate the LAC of different bone tissues at 511 keV. The results had 1.1% error at maximum compared to true values. To test the precision, the effect of 10% variation in effective energy was investigated. In different bone tissues, maximum errors induced by the pricewise linear and hybrid methods were 8.0% and 14.6%, respectively; whereas in the proposed multi-energy method, errors was 1.6%, at maximum.**

I. Introduction

CT-based attenuation correction (CTAC) in clinical hybrid PET/CT scanners plays an important role in improving the quantitative accuracy of PET data. It is well known that the attenuation of photons in the object under study in PET imaging highly influence the accuracy of quantitative PET imaging. Emerging use of CT images in attenuation correction is based on the fact that CT images essentially provide attenuation map i.e. spatial distribution of linear attenuation coefficients (LAC). However, the LACs measured with CT are calculated at the x-ray energy rather than at the 511 keV. It is therefore necessary to perform energy mapping process in which the LACs extracted from the CT images are converted to those corresponding to the 511 keV. Well-established energy mapping techniques, including scaling [1], segmentation [2], hybrid segmentation/scaling [3], piecewise scaling [4,5] and dual-energy decomposition [6] methods have been proposed to determine attenuation map at 511 keV, which are used for attenuation correction and improving the accuracy of regional uptake in PET scanners. Reliability of an attenuation correction method depends on the robustness of the algorithm which is used to determine the attenuation map at 511 keV.

Nowadays, multi-energy x-ray imaging receives emerging attention in the literatures. Most recent improvement in detector technology [7] would promises a new horizon in multi-energy computed tomography and beneficial outcomes in diagnostic imaging. The multi-energy approach would provide an opportunity to calculate elemental composition of body tissues [8]. Recently, efforts have been made to develop multi-energy CT to acquire higher quality tomographic images [9-11]. Interest in using multi-energy imaging is based on its ability in material determination and tissue decomposition; however, achieving reliable and robust outcomes in multi-energy CT strongly depends on the technology and algorithms that are implemented.

Multi-energy measurement in CT imaging may lead to extract more information from scanning object and as a result, could be useful in performing more accurate attenuation correction of PET data. Current CTAC techniques in PET/CT have some drawbacks. The first and most important disadvantages of currently available technique is the error which is induced due to the fact that CT data acquisition is normally performed in the integral detector mode and disregards the energy of photons contributing from the polychromatic x-ray spectrum. The consequence of using polychromatic x-ray in CT is the beam hardening effect which impairs absolute measurement of attenuation coefficients [12].

H. Ghadiri is with the Department of Medical Physics and Biomedical Engineering, and Research Center for Science and Technology in Medicine, Tehran University of Medical Sciences, Tehran, Iran.

M. B. Shiran is with the Department of Medical Physics and Biomedical Engineering, Tehran University of Medical Sciences, Tehran, Iran.

M. R. Ay is with the Department of Medical Physics and Biomedical Engineering, Research Center for Science and Technology in Medicine, and Research Institute for Nuclear Medicine, Tehran University of Medical Sciences, Tehran, Iran. Email: mohammadreza_ay@tums.ac.ir

H. Soltanian-Zadeh is with CIPCE at the Department of Electrical and Computer Engineering, University of Tehran, Tehran, Iran and the Department of Radiology, Henry Ford Health System, Detroit, Michigan, USA.

A. Rahmim is with the Departments of Radiology, and Electrical & Computer Engineering, Johns Hopkins University, Baltimore, Maryland, USA.

H. Zaidi is with the Division of Nuclear Medicine, Geneva University Hospital, Geneva, Switzerland and Geneva Neuroscience Center, Geneva University, Geneva, Switzerland.

978-1-4673-0120-6/11/$26.00 ©2011 IEEE

Whereas, multi-energy CT is suppose to use energy sensitive or photon counting detectors. Secondly, the most proposed energy mapping approaches generally consider the values of LACs or Hounsfield Units (HU) of water and specific tissue (i.e. bone) at the energy of CT and PET and then a linear transformation function is obtained for conversion. The question always arises as to which tissue/parameter should be used to generate the coefficients of energy mapping conversion equations. For example, in hybrid segmentation/scaling method, attenuation coefficient ratios of water and a typical cortical bone in CT and PET energy were used, and in piecewise linear methods although the impact of CT effective energy was decreased by substituting of original attenuation coefficients with HU, using a typical normal bone (e.g. water-cortical assumption) remains as a reference to calculate the scaling coefficients. Nevertheless, complexity and variety of bone tissues in the human body as well as pathologic/oncologic effects which may unpredictably impacts the density and mineral contents of bones require accurate determining of bone tissues. One promising method for more accurate tissue characterization is multi-energy x-ray imaging which could provide a reliable energy mapping basis.

In this study we proposed a new approach for generation of attenuation map in 511 keV based on using multi-energy CT imaging. This method certainly can be used in future generation PET/CT scanners when using CT module with energy sensitive detector technology. The main advantage of the proposed method in comparison with currently available algorithms is the independency of the method with variation in HU values due to aging of x-ray tube and/or detector calibration.

II. Materials and Methods

A. Multi-Energy Conversion Theory

A least squares method for fitting a power function to the LAC values of water and wide range of body tissues (e.g. adipose, marrow, muscle, bone, etc.) was considered as below,

$$LAC(E) = \alpha E^{\beta} + \gamma \qquad (1)$$

in cm^{-1}, where E is the energy, and α, β and γ are the constants to be determined. We have found that by using (1) in the photon energy range from 20 to 150 keV the R-squared error was less than 1%. A variety of bone tissues in the human body, which we assume to be constituted by cortical and marrow mixtures, was also modeled by (1). For all bone tissues the R-squared errors were less than 1% as well.

It is well-known that the elemental composition of materials is the most important determinant of the attenuation coefficient and of the variation of LAC vs. energy [13]. For instance, one of the factors that influence the behavior of LAC vs. energy is the existence of high atomic number elements because of dominant contribution of photoelectric and coherent effects in such cases. One strategy for quantification of the behavior of LAC vs. energy is to determine the declivity of the corresponding curve. It can be shown that the higher the atomic number of the elements (e.g. Calcium and Phosphor in the bone), the more acute decline in the curve of LAC vs. energy [13]. In fact, one of the reliable features that can be extracted from the LAC vs. energy curve could be the *slope* of a tangent line passing through the point $(E_1, LAC(E_1))$ on the curve, which mathematically describes the declivity or the LAC rate of change vs. energy at a given energy E_1:

$$slope = \acute{LAC}(E_1) = \alpha\beta {E_1}^{(\beta-1)} \qquad (2)$$

where prime represents the first derivative of function and E_1 is the specific energy that in practice could be optimized according to the available x-ray spectrum and detector specifications. As a result, from the multi-energy CT measurements, we generate a unique quantity that we label the *slope* (Fig 2).

B. Energy Mapping Based on Multi-Energy Analysis

We postulate and subsequently demonstrate that for conversion from multi-energy CT images to attenuation map at PET energy, a linear conversion equation between the *slope* values and the LAC at 511 keV can be derived as below,

$$LAC(511keV) = a * slope + b \qquad (3)$$

where a and b are constants.

As a result, in a process of energy mapping based on multi-energy CT, two steps should be performed: First, utilizing the pixel values in the multi-energy images to generate *slope* quantities across the image by using equation (2) (resulting in a *slope* map); second, converting the *slope* values to LAC at 511 keV by using the linear conversion equation (3); as illustrated in Fig 2.

C. Simulation

Human shaped phantom including soft tissues and different types of bones were used as an examining object. Software including XCAT phantom [18] for anatomical basics and a series of MATLAB (MathWorks, Inc.) programs for image reconstruction and related calculation was implemented to create series of x-ray fan-beam projections and filtered back projection (FBP) algorithm.

Simulation of bone tissues were performed using materials mixtures method. Variety of bone substitutes have been simulated and analyzed by authors in the implementation of the energy mapping algorithms, including water-cortical [4, 5] and water-K_2HPO_4 [14] mixtures. We assumed that bone is an additive mixture of cortical, red marrow and yellow marrow constituents. A wide range of cortical concentrations in equal volumetric fractions of red and yellow marrow was considered in order to construct a full range of human bone tissue. Explicitly,

$$f_{co} + f_{rm} + f_{ym} = 1 \qquad (4)$$

and

$$\rho_M = f_{co}\rho_{co} + f_{rm}\rho_{rm} + f_{ym}\rho_{ym} \qquad (5)$$

where ρ and f are mass density and volumetric fraction, subscripts *M*, *co*, *rm* and *ym* denote the mixture, cortical, red marrow and yellow marrow materials, respectively, and $f_{rm} = f_{ym}$. Considering the general mixture method [13], stating that the attenuation coefficient of a mixture can be calculated from the attenuation coefficients of its constituents

and the corresponding fractions, the LAC of a mixture can be expressed as,

$$LAC_M = \left(MAC_{co}\rho_{co}f_{co} + MAC_{rm}\rho_{rm}f_{rm} + MAC_{ym}\rho_{ym}f_{ym}\right) \quad (6)$$

where MAC is the mass attenuation coefficient.

In order to simulate wide range of bone tissues of the human body, we varied f_{co} from 0.0 to 1.0. The values of f_{rm} and f_{ym}, using $f_{rm} = f_{ym}$, were calculated by using (4), and the corresponding LACs were then derived by using (6). The MAC of the cortical bone, red marrow and yellow marrow materials were calculated by using the WinXCom program [15] considering the elemental weight compositions reported in [16] (Table I).

TABLE I. ELEMENTAL COMPOSITION (% BY MASS) AND MASS DENSITY OF THE CORTICAL BONE, RED MARROW AND YELLOW MARROW MATERIALS [16].

	Cortical	Red marrow	Yellow marrow
w_H	3.4	10.5	11.5
w_C	15.5	41.4	64.4
w_N	4.2	3.4	0.7
w_O	43.5	43.9	23.1
w_P	10.3	0.1	0.0
w_{Ca}	22.5	0.0	0.0
w_{other}	0.60	0.70	0.30
$\rho\ (g/cm^3)$	1.92	1.03	0.98

To obtain a general energy mapping equation, the LACs were calculated for a wide range of bone tissues at an energy range of 20 to 140 keV by using (4)-(6). For each bone tissue the *slope* value was obtained by using (1) and then (2) at a specific energy E_1 (different E_1 values of 30, 40, 50, 60 and 70 keV were considered). The *slope* values were then plotted against LAC at 511 keV of the corresponding bone tissues, and a least square curve fitting technique was then utilized to derive the constants of the linear conversion equation (3).

To quantify the accuracy of the energy mapping algorithm based on multi-energy CT, the energy spectrum of a 140 kVp photon beam with *1 mm Al* equivalent inherent filtration was used. An energy sensitive detector was considered with ideal energy resolution and quantum efficiency.

The detected photons were divided into 5 bins with average energies of 30, 50, 70, 90 and 110 keV. Then for each bin the projected data were reconstructed into the tomographic image.

Multi-energy images were then overlaid and packed into a two dimensional matrix, in which each element was a vector $L_{m,n}$ comprised of LAC values in 5 energy bins, as below,

$$L_{m,n}=(l_1, l_2, l_3, l_4, l_5) \quad (7)$$

where m and n are pixel coordinates (as row and column numbers), and l_i denotes the LAC in ith energy bin.

For all m and n, the LACs variation vs. energy of bins within $L_{m,n}$ vectors using the proposed power function (1) were modeled and the *slope* values, as defined in (2), were calculated and the *slope* map was obtained (Fig 2c). The *Slope* map is essentially an image which represents the distribution of *slope* quantities corresponding to m and n coordinates. The attenuation map was then estimated by using the linear equation (3).

The LACs at 511 keV for four regions including: Spongiosa, Innominate, Mandible and Femur shaft bone tissues of human body, with their characteristics reported in [15, 16], were particularly computed by exploiting the proposed energy mapping algorithm in this study.

To investigate the stability of proposed energy mapping method in the case of scant precision in Hounsfield Unit/LAC measurement, an intentional 10% error was induced to estimated effective energy values. Resultant percentage errors in multi-energy method for four different bone tissues were calculated and compared to hybrid and piecewise linear energy mapping algorithms.

III. RESULTS

The energy mapping conversion curves for E_1=30, 40, 50, 60 and 70 keV are plotted in Fig 1. One may conclude that a choice of lower E_1 value is more sensitive to different bone types, as it offers a greater span of slope values (see discussion in Sec. IV). For E_1=*30* and *40* keV, the constant of (3) were derived as *a=-0.37, b=0.092* and *a=-1.133, b=0.091*, respectively.

Table II shows the fitted α, β and γ constant values in (1) for four bone tissues (Spongiosa, Innominate, Mandible and Femur shaft) and the corresponding *slope* values for these bone tissues as calculated by (2).

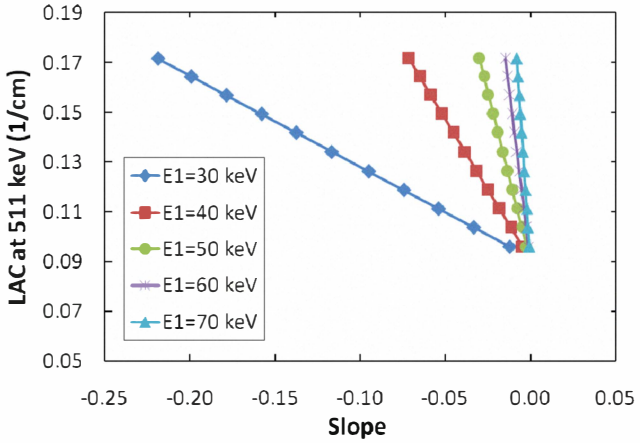

Fig 1. Conversion graph from multi-energy CT images to LAC at 511 keV, for different E_1 values calculated for full scale of bone tissues.

TABLE II. FITTED POWER FUNCTION COEFFICIENTS, SLOPES VALUES FOR E_1=40 KEV, ESTIMATED LAC AT 511 KEV AND THE PERCENTAGE ERROR FOR FOUR DIFFERENT BONE TISSUES.

	Spongiosa	Innominate	Mandible	Femur shaft
α	7528.2	18542.2	28978.1	33448.8
β	-2.78	-2.85	-2.88	-2.88
γ	0.19	0.22	0.25	0.26
Slope	-0.0185	-0.0355	-0.0511	-0.0578
LAC511 (estimated)	0.1104	0.1297	0.1473	0.1549
LAC511 (actual)	0.1117	0.1309	0.1486	0.1561
Error %	1.1	0.90	0.9	0.80

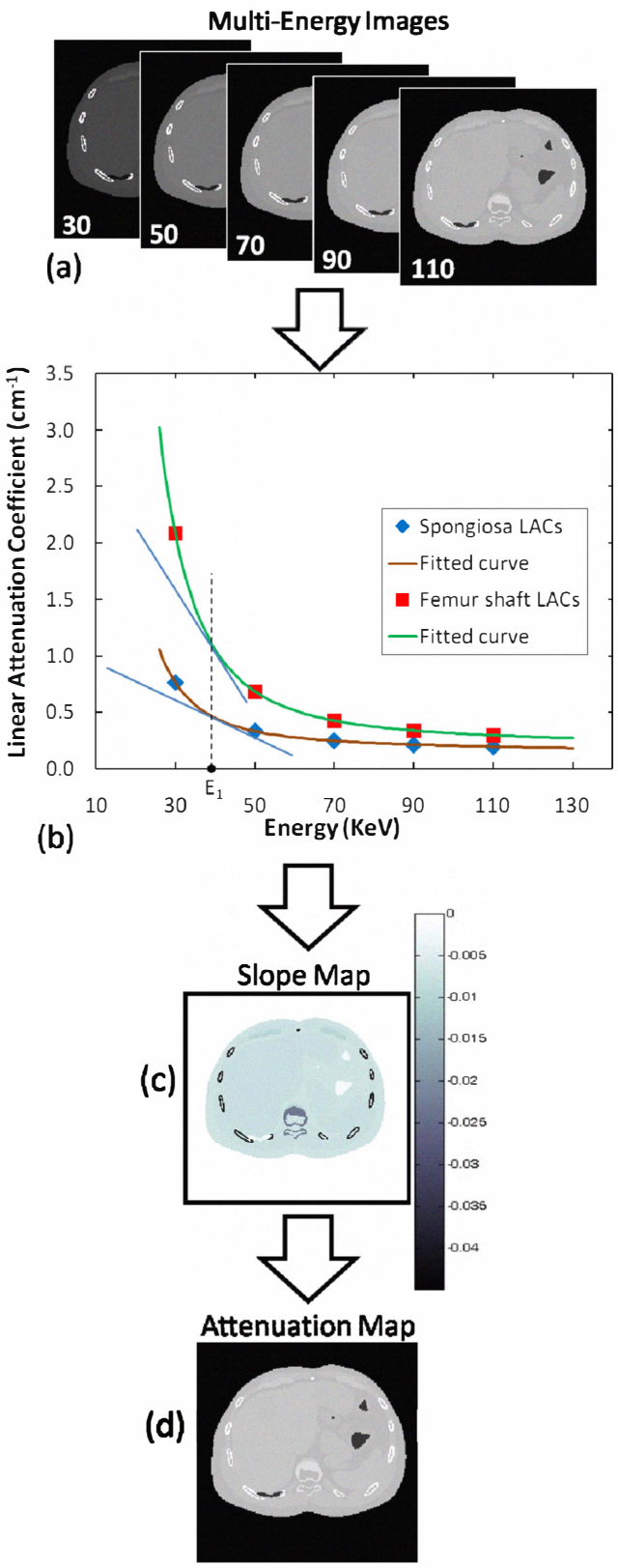

Fig 2. Energy mapping algorithm flow chart based on multi-energy CT. a) Simulated multi-energy images at different energy bins. b) LAC vs. energy values for regions belongs to Spongiosa and Femur shaft bones and fitted curves. The tangent lines at $E = E_1$ were also plotted. c) Slope map. d) 511 keV attenuation map.

The estimated LACs at 511 keV were obtained by using the linear equation (3) as,

$$LAC(511keV) = -1.33 * slope + 0.09 \qquad (8)$$

and the percentage errors were compared to actual values derived from the literatures [15-17], all of which are also listed in Table II.

The errors due to 10% inaccuracy in HU/LAC measurement in multi-energy, piecewise linear and hybrid energy mapping methods are compared in table III.

TABLE III. PERCENTAGE ERROR IN ESTIMATED LAC AT 511 KEV DUE TO 10% ERROR IN EFFECTIVE ENERGY CALCULATION IN TWO PIECEWISE LINEAR (PL) METHODS, HYBRID SEGMENTATION/SCALING (HY) AND MULTI-ENERGY (ME) ALGORITHMS.

Method	Percentage Error (%)			
	Spongiosa	Innominate	Mandible	Femur shaft
ME	1.6	1.4	1.3	1.2
PL [5]	3.3	5.6	7.5	8.1
PL [4]	2.7	4.6	5.9	6.4
HY [3]	2.4	14.6	10.9	9.5

IV. DISCUSSION

The aim of this study was to propose an energy mapping algorithm based on multi-energy CT imaging. This algorithm consists of two main steps: first, abstracting multi-energy images to a preliminary map of *slopes* values; second, exploiting an energy mapping conversion equation to transform the *slope* map to attenuation map at 511 keV. The first step is based on the assertion that accurate determination of the attenuation coefficient at 511 keV in bone tissues benefits from multi-energy observation. This is due to the fact that LAC is a function of three main parameters: energy, atomic number and density, while the last two parameters may independently change. Consequently, measuring HU/LAC at a single effective energy induces two kinds of error due to the calculation of effective energy from a wide spectrum of x-rays, and lack of knowledge regarding exact mineral contents. Therefore, defining a feature that could represent LAC variation vs. energy, i.e., *slope*, could better aid in the determination of tissue characteristics. The second step asserts that more exact determination of mineral content and density of bones leads to more accurate energy mapping. For this, a bone model composed of the cortical bone and marrow with very close chemical and physical characteristics to real bone tissues was considered, and a general linear energy mapping conversion equation was obtained based on this model.

Characteristic factors i.e. elemental composition, mass density and effective atomic number of human bone tissues were modeled by mixtures of cortical bone and marrow materials in which the marrow contained 50% red and 50% yellow marrow. Calculated ρ_M and LAC_M by using (5) and (6) revealed that the mixture of the cortical bone and marrow not only mimicked the elemental composition of a variety of human bones, but also the mass density had good agreement with published data in [16, 17]. As it was demonstrated that the effective atomic number of any material can be calculated

by using its elemental mass weights [13], consequently, our proposed bone model could also mimic effective atomic number of human bone tissue because of its ability in generating elemental compositions weights (by mass) very close to real values.

The proposed mathematical function in this study shows that LAC variation of human body tissues vs. energy can be modeled by a power equation like (1) with small error, especially in bone tissues. The total squared error in curve fitting for muscle, red marrow, yellow marrow and cortical bone was 1% maximum in the range of 20 to 150 keV.

To extract the constant values in the linear energy mapping equation of (3), a specific energy E_1 must be selected. Both x-ray quality and detector specifications affect the energy span of photons; therefore, it requires some care to select specific energy E_1. To maximize the sensitivity of *slope* to mineral contents and density, a small and achievable energy within the band of filtered x-ray spectrum must be selected for E_1. For lower E_1 values, a wider span of slopes was obtained for the range of materials studied (Fig 1), indicating greater sensitivity and subsequent ability for accurate conversion to LAC at 511keV. On the other hand, a mere *1 mm Al* equivalent intrinsic filtration in a tungsten-targeted x-ray tube, eliminates most of the x-ray photons with energies less than 15 keV from spectrum generated by 150 kVp potential. Furthermore, when the surviving photons pass 25 cm of water, the photons with energies less than 25 keV are mostly attenuated. Considering at least a 20 keV energy window width for each bin and 25 keV as the minimum feasible energy of photons in the x-ray spectrum, the first feasible point on the curve of LAC vs. energy, to be selected as E_1, must be greater than 30 keV. Although it is analytically feasible to select E_1 to be much smaller, but to make our algorithm more applicable we preferred to emphasize on the setting E_1=40 keV. In any case, E_1 must be optimized according to the particular x-ray spectrum and detector specifications.

As mentioned in Table II, the LACs at 511 keV as estimated by the energy mapping method proposed in this paper showed good agreement with actual values. This can be attributed to the high sensitivity of the *slope* to the tissue's physical and chemical characteristics. The *slope* quantity, derived from the first derivative of the LAC vs. energy curve, represents the rate of variation of LAC in a specific energy. It is well known that the LAC of materials with higher atomic number and/or higher densities shows more acute decline in LAC vs. energy curve. As such, quantification of such declivity may lead to higher sensitivity to tissue characteristics, and as a result, more reliable energy mapping.

It is worth noting that in some circumstances the HU or effective energy in CT may undesirably change due to aging of the x-ray tube [19] and its replacement, and modulations in detector performance. The basic parameter used in the hybrid segmentation/scaling method [3] is the effective energy, and HU at a specific kVp is also the basic parameter in the piecewise linear scaling method [4, 5]. Any inaccuracy in the derivation of these parameters, either subjectively or objectively, leads to unreliable attenuation maps. As shown in Table III, the algorithm proposed in this study reveals better stability and less dependency to such induced errors. This promising stability and independency is because of the fact that it is the trend of LAC variation that contributes in our calculation (and not its absolute scale). The trend of LAC variation vs. energy is less dependent to the selected energies, so the *slope* values as used in our proposed multi-energy method was hardly affected by the above mentioned errors. To investigate such behavior, an intentional error of 10% was considered on the effective energy of x-ray spectrum. The hybrid method was significantly influenced by the induced error because of its high and direct dependency on the effective energy. The piecewise linear method seemed to be less affected than the hybrid method, but still significantly. This could be due to less dependency to effective energy because of using HU instead of LAC in the calculation process. The least affected method was the proposed multi-energy method in this study which could be due to its basic parameter independency.

V. Conclusion

The algorithm proposed in this paper accurately estimates the LAC at 511 KeV in a wide range of bone tissues in the human body. Unlike algorithms based on integrated energy CT, which show some level of instability due to errors in the HU/effective energy determination, using multi-energy CT could be a promising solution for stable and reproducible energy mapping in CTAC. Less dependency of the proposed energy mapping technique to HU/effective energy variations, which normally occur in calibration procedure, as compared to hybrid and piecewise linear methods, was shown to improve the accuracy over conventional energy mapping methods especially for bones.

References

[1] T. Beyer, P. E. Kinahan, D. W. Townsend, D. Sashin, "The use of x-ray CT for attenuation correction of PET data", *Proc. IEEE Nuclear Science Symposium and Medical Imaging Conference*, vol. 4, pp. 1573–1577, Nov 1994.

[2] P. E. Kinahan, B. H. Hasegawa, T. Beyer, "X-ray-based attenuation correction for positron emission tomography/computed tomography scanners", *Semin. Nucl. Med.*, vol. 33, no. 3, pp. 166–179, Jul 2003.

[3] P. E. Kinahan, D. W. Townsend, T. Beyer, D. Sashin, "Attenuation correction for a combined 3D PET/CT scanner", *Med. Phys.*, vol. 25, no. 10, pp. 2046–2053, Oct 1998.

[4] C. Bai, L. Shao, A. J. Da Silva, and Z. Zhao, "A Generalized model for the conversion from CT numbers to linear attenuation coefficients", *IEEE Trans. Nucl. Sci.*, vol. 50, no. 5, pp. 1510-1515, Oct 2003

[5] C. Burger, G. Goerres, S. Schoenes, A. Buck, A.H.R. Lonn, G.K. von Schulthess, "PET attenuation coefficients from CT images: experimental evaluation of the transformation of CT into PET 511 keV attenuation coefficients", *Eur. J. Nucl. Med. Mol. Imaging,* vol. 29, no. 6, pp. 922-927, Jul 2002.

[6] P. E. Kinahan, A. M. Alessio, J. A. Fessler, "Dual energy CT attenuation correction methods for quantitative assessment of response to cancer therapy with PET/CT imaging", *Technol. Cancer. Res. Treat.,* vol. 5, no. 4, pp. 319–327, Aug 2006.

[7] S. Del Sordo, L. Abbene, E. Caroli, A. M. Mancini, A. Zappettini, P. Ubertini, "Progress in the Development of CdTe and CdZnTe Semiconductor Radiation Detectors for Astrophysical and Medical Applications", *Sensors* , vol. 9, no. 5, pp. 3491–3526, May 2009.

[8] S. M. Midgley, "Materials analysis using x-ray linear attenuation coefficient measurements at four photon energies", *Phys. Med. Biol.*, vol. 50, no. 17, pp. 4139–4157, Sep 2005.
[9] P. M. Shikhaliev, "Energy-resolved Computed tomography: first experimental results", *Phys. Med. Biol.*, vol. 53, no. 20, pp. 5595-5613, Sep 2008.
[10] J. P. Schlomka *et al*, "Experimental feasibility of multi-energy photon-counting K-edge imaging in pre-clinical computed tomography", *Phys. Med. Biol.*, vol. 53, no. 17, pp. 4031–4047, Jul 2008.
[11] M. F. Walsh *et al,* "First CT using Medipix3 and the MARS-CT-3 spectral scanner", *JINST*, vol. 6, C01095, no. 01, Jan 2011.
[12] H. Zaidi, M. L. Montandon, and A. Alavi, "Advances in attenuation correction techniques in PET", *PET Clinics*, vol. 2, no. 2, pp. 191-217, 2007.
[13] F. W. Spiers, "Effective atomic number and energy absorption in tissues", *Br. J. Radiol.*, vol. 19, pp. 52-63, 1946.
[14] M. R. Ay, M. Shirmohammad, S. Sarkar, A. Rahmim, and H. Zaidi, "Comparative assessment of energy-mapping approaches in CT-based attenuation correction for PET", *Mol. Imaging Biol.,* Vol. 13, no. 1, pp. 187-198, 2010.
[15] L. Gerward, N. Guilbert, K.B. Jensen, and H. Levring,"WinXCom – a program for calculating X-ray attenuation coefficients", *Radiat. Phys. Chem.*, vol. 71, no. 3-4, pp. 653–654, 2004.
[16] International Commission on Radiation Units and Measurements, "Tissue substitutes in radiation, dosimetry and measurement", *ICRU*, Report 44, Bethesda, MD, 1989.
[17] H. Q. Woodard, D. R. White, "Bone models for use in radiotherapy dosimetry", *Br. J. Radiol.*, vol. 55, no. 652, pp. 277-282, 1982.
[18] W. P. Segars, M. Mahesh, T. J. Beck, E. C. Frey, and B. M. W. Tsui, "Realistic CT simulation using the 4D XCAT phantom", *Med. Phys.*, vol. 35, no. 8, pp. 3800-3808, Aug 2008.
[19] A. Mehranian, M. R. Ay, N. R. Alam, H. Zaidi, "Quantifying the effect of anode surface roughness on diagnostic x-ray spectra using Monte Carlo simulation", *Med. Phys.*, vol. 37, no. 2, pp. 742-752, Feb 2010.